Connexin30.2 containing gap junction channels decelerate impulse propagation through the atrioventricular node

Maria M. Kreuzberg*†, Jan W. Schrickel†‡, Alexander Ghanem‡, Jung-Sun Kim§, Joachim Degen*, Ulrike Janssen-Bienhold¶, Thorsten Lewalter‡, Klaus Tiemann‡, and Klaus Willecke*‖

*Institut für Genetik, Abteilung Molekulargenetik, Universität Bonn, Römerstrasse 164, 53117 Bonn, Germany; ‡Medizinische Klinik und Poliklinik II, Universitätsklinikum Bonn, Sigmund-Freud Strasse 25, 53105 Bonn, Germany; §Department of Pathology, Asan Medical Center, University of Ulsan, Pungnap-dong, Songpa-gu, Seoul 388-1, Korea; and ¶Neurobiologie, Institut für Biologie und Umweltwissenschaften, Fakultät V, Universität Oldenburg, 26111 Oldenburg, Germany

Edited by Michael V. L. Bennett, Albert Einstein College of Medicine, Bronx, NY, and approved February 2, 2006 (received for review September 29, 2005)

In the mammalian heart, gap junction channels between electrically coupled cardiomyocytes are necessary for impulse propagation and coordinated contraction of atria and ventricles. Recently, mouse connexin30.2 (Cx30.2) was shown to be expressed in the cardiac conduction system, predominantly in sinoatrial and atrioventricular (AV) nodes. The corresponding gap junctional channels expressed in HeLa cells exhibit the lowest unitary conductance (9 pS) of all connexin channels. Here we report that Cx30.2 slows down the propagation of excitation through the AV node. Mice expressing a LacZ reporter gene instead of the Cx30.2 coding region (Cx30.2$^{LacZ/LacZ}$) exhibit a PQ interval that is ≈25% shorter than in WT littermates. By recording atrial, His, and ventricular signals with intracardiac electrodes, we show that this decrease is attributed to significantly accelerated conduction above the His bundle (atrial-His interval: 27.9 ± 5.1 ms in Cx30.2$^{LacZ/LacZ}$ versus 37.1 ± 4.1 ms in Cx30.2$^{+/+}$ mice), whereas HV conduction is unaltered. Atrial stimulation revealed an elevated AV-nodal conduction capacity and faster ventricular response rates during induced episodes of atrial fibrillation in Cx30.2$^{LacZ/LacZ}$ mice. Our results show that Cx30.2 contributes to the slowdown of impulse propagation in the AV node and additionally limits the maximum number of beats conducted from atria to ventricles. Thus, it is likely to be involved in coordination of atrial and ventricular contraction and to fulfill a protective role toward pathophysiological states such as atrial tachyarrhythmias (e.g., atrial fibrillation) by preventing rapid conduction to the ventricles potentially associated with hemodynamic deterioration.

atrial fibrillation | cardiac connexins | conductive myocardium | coordinated cardiac contraction

Gap junctions are intercellular conduits that allow direct communication between neighboring cells. Two hemichannels, one contributed by each adjacent cell, form a pore that permits diffusion of ions, metabolites, and peptides <1.8 kDa molecular mass (1, 2). The protein subunits of these channels are the connexins (Cx) that are encoded by a multigene family, including 20 members in mice (3).

It has been known for several years that three different connexins, i.e., Cx40, Cx43, and Cx45, are expressed by cardiac myocytes. The corresponding gap junctional channels are involved in electrical impulse propagation and coordinated contraction of the heart (4). The expression of these connexins is restricted to specialized compartments: Cx43 is the major connexin in the working myocytes of atria and ventricles (5, 6); Cx40 is detected in the atrioventricular (AV) conduction system and in atrial working myocytes (7, 8). Cx45 is abundantly expressed in the sinoatrial (SA) node and the AV conduction system (9–11).

Generation of Cx-deficient mice for Cx40, Cx43, and Cx45 helped to elucidate the involvement of these connexins in proper heart function. Targeted deletion of Cx40 in mice resulted in right bundle branch block and impaired left bundle branch conduction (7). The unrestricted ablation of Cx43 in mice caused postnatal death as a consequence of major heart defects (6). Cx43 conditional knockout mice with induced deletion of Cx43 in the heart exhibited reduced conduction velocity, increased dispersion of conduction, and enhanced electrical vulnerability on the ventricular level (12). The unrestricted ablation of Cx45 resulted in an embryonic lethal phenotype due to major defects in vascularization (11). Conditional deletion of Cx45 in the heart could not circumvent embryonic lethality (13).

We recently reported Cx30.2 to be a new cardiac connexin in mice that is predominantly expressed in the cardiac conduction system, especially in the nodal regions (14). We suggested that Cx30.2 channels with their low unitary conductance of only 9 pS, i.e., the lowest among the connexin gene family, might contribute to the decrease of conduction velocity within the AV node of the conduction system (14).

To get further insights into the biological function of Cx30.2 in mice, we have conditionally replaced the Cx30.2 coding region by a LacZ reporter gene (Cx30.2LacZ). LacZ expression in the cardiac conduction system was accompanied by a lack of Cx30.2 immunoreactivity in the respective area and, thus, demonstrated the ablation of Cx30.2. Functional analyses of fertile Cx30.2-deficient mice revealed accelerated AV-nodal conduction velocity in the knockout mice.

Results

Generation of a Cx30.2$^{LacZ/LacZ}$ Mice. To circumvent possible lethality of Cx30.2 null mice, we generated conditional Cx30.2-deficient mice. In these mice, cell type-specific or an unrestricted deletion of the Cx30.2 coding region could be obtained by activity of Cre recombinase, resulting in expression of the LacZ reporter gene under control of Cx30.2 gene regulatory elements.

ES cells were transfected with the targeting vector, and homologous recombination in the resulting clones was tested by PCR and Southern blot analyses (data not shown). Blastocyst injection of three homologously recombined ES cell clones yielded germ-line transmission chimeras that produced heterozygous Cx30.2$^{+/fl}$ offspring after breeding with C57BL/6 mice.

Cx30.2$^{+/fl}$ mice were mated to hACTB:FLPe mice (15) to generate Cx30.2$^{+/fldN}$ animals that were deprived of the selection

Conflict of interest statement: No conflicts declared.

This paper was submitted directly (Track II) to the PNAS office.

Abbreviations: A, atrial electrogram; AV, atrioventricular; Cx, connexin; H, His signal; SA, sinoatrial; V, ventricular electrogram.

†M.M.K and J.W.S. contributed equally to this work.

‖To whom correspondence should be addressed. E-mail: genetik@uni-bonn.de.

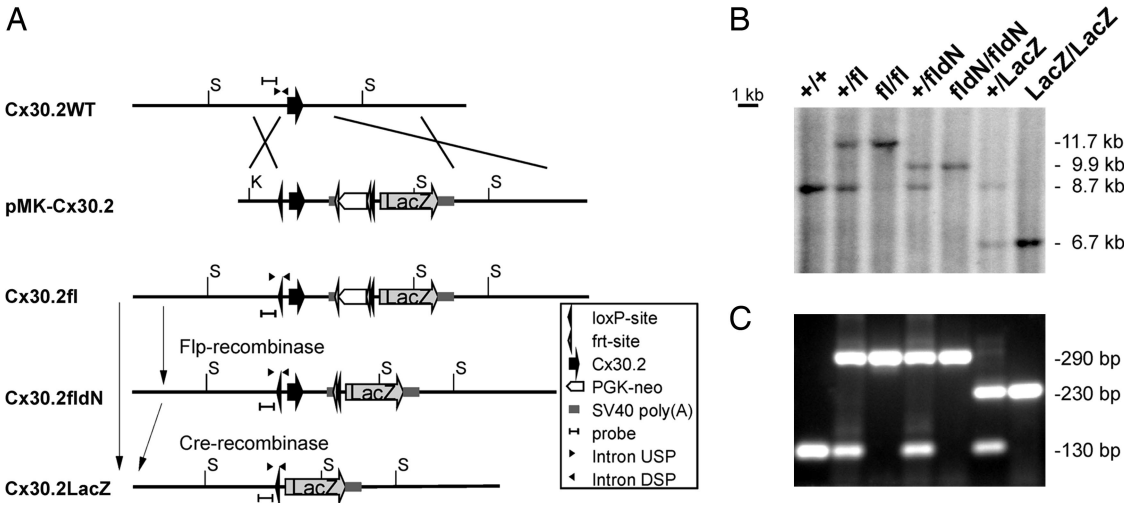

Fig. 1. Generation of Cx30.2-deficient mice with LacZ reporter gene (Cx30.2$^{LacZ/LacZ}$). (*A*) Targeting scheme. Transfection of HM1-cells and homologous recombination of the pMK-Cx30.2 targeting vector yielded heterozygous cells containing a Cx30.2fl allele. Blastocyst injection of homologously recombined ES cells results in germ-line transmission chimeras that give offspring to Cx30.2$^{+/fl}$ mice after mating to C57BL/6 animals. Breeding of Cx30.2$^{+/fl}$ mice and hACTB:FLPe mice generates Cx30.2$^{+/fldN}$ mice harboring a Cx30.2fldN allele that was deprived of the PGK-neo selection cassette (indicated as dN) after Flp mediated recombination. Crossing of Cx30.2$^{+/fl}$ or Cx30.2$^{+/fldN}$ mice to PGK-Cre mice resulted in Cx30.2$^{+/LacZ}$ mice caused by Cre-recombinase-mediated deletion of the loxP-sites flanked region. (*B*) Southern blot analysis with an internal probe derived from the 5′ homologous region. SacI digestion of liver DNA from animals with different allelic combinations resulted in detection of an 8.7-kb fragment for the Cx30.2WT allele, 9.9-kb fragment for the Cx30.2fldN allele, 11.7-kb fragment for the Cx30.2fl allele, and a 6.7-kb fragment for the Cx30.2LacZ allele. (*C*) PCR genotyping of the corresponding animals. The Cx30.2-specific primer combination amplified from the Cx30.2WT allele an 130-bp fragment, from the Cx30.2fl and the Cx30.2fldN allele a 290-bp fragment, and from the Cx30.2LacZ allele a 230-bp fragment.

cassette (indicated as dN) after frt/Flp-mediated removal (Fig. 1*A*). Breeding of Cx30.2$^{+/fl}$ or Cx30.2$^{+/fldN}$ mice with PGK-Cre mice (16) resulted in Cx30.2$^{+/LacZ}$ mice after unrestricted Cre-mediated recombination (Fig. 1*A*). Cx30.2-deficient animals (Cx30.2$^{LacZ/LacZ}$) were born at the expected Mendelian frequency and turned out to be fertile. The different genotypes were proven by PCR (Fig. 1*B*) and Southern blot analyses (Fig. 1*C*). After hematoxylin/eosin staining of paraffin slices, no obvious differences in heart morphology or size and structure of the AV node could be observed between the Cx30.2$^{+/+}$ and Cx30.2$^{LacZ/LacZ}$ animals (data not shown).

Cx30.2 and LacZ Reporter Gene Expression. To determine the functionality of the LacZ reporter gene, we investigated Cx30.2 and LacZ expression at RNA and protein levels in the heart. Intron-spanning RT-PCR analyses of the different genotypes Cx30.2$^{+/+}$, Cx30.2$^{+/LacZ}$, and Cx30.2$^{LacZ/LacZ}$ revealed Cx30.2 transcripts only in Cx30.2$^{+/+}$ and Cx30.2$^{+/LacZ}$ mice as expected, whereas LacZ transcripts were found in Cx30.2$^{+/LacZ}$ and Cx30.2$^{LacZ/LacZ}$ mice (Fig. 4, which is published as supporting information on the PNAS web site). Immunofluorescence analyses with Cx30.2 antibodies revealed Cx30.2 expression in the AV node in Cx30.2$^{+/+}$ and Cx30.2$^{+/LacZ}$ mice (Fig. 2 *A* and *B*). No signals were found in Cx30.2$^{LacZ/LacZ}$ animals (Fig. 2*C*). In Cx30.2$^{+/LacZ}$ mice, the immunofluorescence signals were colocalized with LacZ staining in consecutive slices, demonstrating the functionality of the LacZ reporter gene (Fig. 2 *B* and *E*).

Additionally, we performed RT-PCR and immunofluorescence analyses in animals harboring the Cx30.2fl or Cx30.2fldN allele to prove the expression of the "floxed" Cx30.2 gene in the conditional-deficient mice. We detected Cx30.2 transcript and protein expression in both allelic variants, although the expression level of the Cx30.2fldN allele was somewhat lower (Fig. 4).

We further investigated the LacZ expression pattern in cryosections of different organs of Cx30.2$^{+/LacZ}$ mice. Besides expression in the AV node, we found LacZ staining in the medulla of the adrenal gland and in different subtypes of neurons in the central nervous system (M.M.K. and K.W., unpublished data).

Echocardiography. Heart rates at rest were similar in Cx30.2$^{+/+}$ and Cx30.2$^{LacZ/LacZ}$ mice and increased in both genotypes adequately during dobutamine stress. Left ventricular volumes and masses were calculated in diastole and revealed no significant differences between controls and Cx30.2$^{LacZ/LacZ}$ mice (Table 3, which is published as supporting information on the PNAS web site). Mean left ventricular enddiastolic volumes at peak dobutamine stress also revealed no significant differences between Cx30.2$^{+/+}$ and Cx30.2$^{LacZ/LacZ}$ animals (Table 3). The ejection fraction at rest was found within normal range for Cx30.2$^{LacZ/LacZ}$ (71 ± 6%) and their WT littermates (74 ± 5%). Both groups demonstrated adequate increase of ejection fraction during dobutamine stress, displaying a similar contractile reserve.

Electrophysiological Investigation. To evaluate the influence of Cx30.2 ablation on impulse propagation and conduction properties, we performed surface ECG analyses and invasive electrophysiological investigation. During the electrophysiological investigation, three Cx30.2$^{LacZ/LacZ}$ mice died because of third-degree AV block that occurred upon positioning of the catheter while passing the tricuspid valve (Fig. 5, which is published as supporting information on the PNAS web site). Two Cx30.2$^{LacZ/LacZ}$ mice developed second-degree AV block during catheter positioning, which was completely reversible after relocalization of the electrophysiological catheter. None of the WT animals displayed such enhanced vulnerability of the AV-nodal region to mechanical challenges, which generally is a rare phenomenon in murine electrophysiological investigation.

Surface ECG and Intracardial Electrograms. While performing ECG analyses (all groups showed identical heart rates under anesthesia), we found a significantly shortened PQ interval in

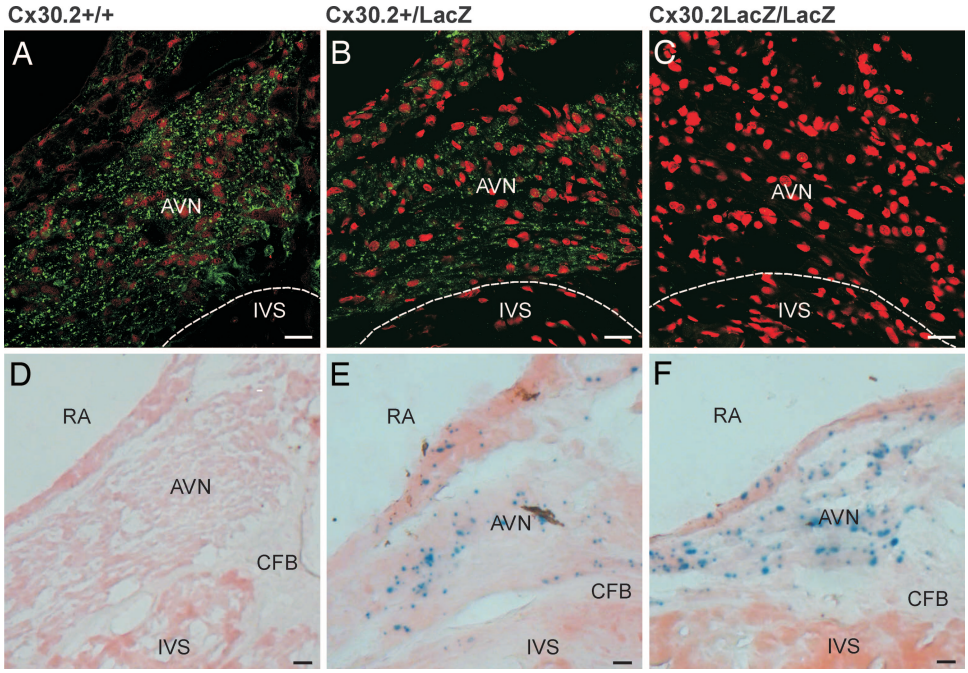

Fig. 2. Immunostaining with Cx30.2-specific antibodies (green) and LacZ staining of consecutive heart sections. (*A* and *D*) AV-nodal cells of Cx30.2$^{+/+}$ mice are immunopositive for Cx30.2 but exhibit no LacZ expression. (*B* and *E*) Cx30.2 immunostaining and LacZ staining of the AV node in Cx30.2$^{+/LacZ}$ mice demonstrate the functionality of the LacZ reporter gene. (*C* and *F*) No Cx30.2 immunostaining is found in the cardiac conduction system of Cx30.2$^{LacZ/LacZ}$ mice that are deficient for Cx30.2, whereas LacZ staining is present. Red shows propidium iodide staining of the nuclei. AVN, atrioventricular node; CFB, central fibrous body; IVS, interventricular septum; RA, right atrium. (Scale bars: 20 μm.)

Cx30.2$^{LacZ/LacZ}$ compared with Cx30.2$^{+/+}$ animals (Table 1). No significant changes were found in P wave duration, QRS width, and QT interval (Table 1).

After positioning of the electrophysiological catheter with its electrodes on atrial and ventricular level, intracardiac electrograms [atrial (A), His (H), and ventricular (V) signal] were recorded and analyzed in all investigated animals (Fig. 3 and Table 1). In analogy to surface ECG, significantly shorter AV intervals, as evidence for accelerated AV-nodal conduction, were documented in Cx30.2$^{LacZ/LacZ}$ animals. Evaluation of AH and HV intervals showed significantly reduced AH durations in Cx30.2-deficient animals, whereas HV intervals were unchanged in Cx30.2$^{LacZ/LacZ}$ versus Cx30.2$^{+/+}$ animals (Table 1). Thus, shortening of the PQ interval in the surface ECG could clearly be attributed to increased supraHisian conductivity indicated by shorter AH intervals, whereas alterations of HV as surrogate parameter for infraHisian conduction were not found.

Table 1. Results of surface ECG and intracardiac electrogram analyses

Analysis	Cx30.2$^{LacZ/LacZ}$	Cx30.2$^{+/+}$	*P*
	Surface ECG		
RR, ms	138.6 ± 25.8	143.9 ± 22.7	0.59
HR, bpm	449 ± 95	426 ± 61	0.46
P, ms	14.6 ± 2.1	15.9 ± 2.2	0.15
PQ, ms	35.0 ± 3.9	47.2 ± 4.9	<0.00001
QRS, ms	14.1 ± 1.7	12.7 ± 2.1	0.11
QT, ms	37.9 ± 3.2	36.6 ± 5.3	0.49
QTc, ms	102.7 ± 8.4	96.9 ± 12.2	0.19
	Intracardiac electrograms		
SCL, ms	131.6 ± 13.8	135.2 ± 25.0	0.70
AV, ms	38.3 ± 4.1	48.4 ± 4.3	0.0002
AH, ms	27.9 ± 5.1	37.1 ± 4.1	0.00003
HV, ms	9.8 ± 1.3	11.2 ± 2.1	0.10

n = 14 and 11 in surface ECG Cx30.2$^{LacZ/LacZ}$ and Cx30.2$^{+/+}$, respectively, and *n* = 11 and 10 in intracardiac electrograms Cx30.2$^{LacZ/LacZ}$ and Cx30.2$^{+/+}$, respectively. RR, interval from R to R-peak; HR, heart rate; PQ, onset of P wave to beginning of Q wave; QRS, beginning of Q wave to the point of the S wave returning to the isoelectrical line; QT, onset of the Q wave to the ending of the T wave; QTc, rate-corrected QT interval; SCL, sinus cycle length.

Transvenous Electrophysiology. Transition of electrical impulses from the atria to the ventricles via the AV node can be estimated

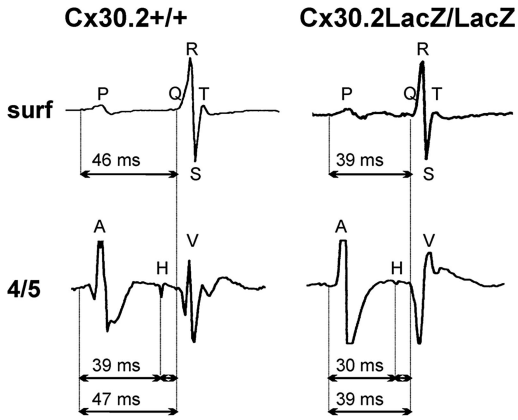

Fig. 3. Comparison of surface ECG and intracardiac electrogram of Cx30.2$^{+/+}$ and Cx30.2$^{LacZ/LacZ}$ littermates. Two examples of representative surface ECG (surf) and intracardiac electrograms at the position of the His bundle (electrode pair: 4/5) are presented. Shorter PQ intervals indicate accelerated AV-nodal conduction. The AH interval in the Cx30.2$^{LacZ/LacZ}$ mouse is shorter at a similar HV interval (9 ms in Cx30.2$^{LacZ/LacZ}$ versus 8 ms in Cx30.2$^{+/+}$) and P wave duration (19 ms versus 21 ms). This example illustrates accelerated supraHisian conduction in Cx30.2$^{LacZ/LacZ}$ mice. AH, interval from atrial to His signal; HV, His signal to first the QRS movement.

Table 2. Transvenous electrophysiological stimulation

Analysis	$Cx30.2^{LacZ/LacZ}$	$Cx30.2^{+/+}$	*P*
	Atrial stimulation		
SNRP (corr. SNRP), ms (S1S1, 120 ms)	167.8 ± 32.0 (37.7 ± 21.3)	190.4 ± 60.1 (51.8 ± 35.3)	0.36 (0.26)
SNRP (corr. SNRP), ms (S1S1, 100 ms)	175.5 ± 39.8 (43.3 ± 31.6)	211.8 ± 63.9 (76.6 ± 73.4)	0.15 (0.21)
SNRP (corr. SNRP), ms (S1S1, 80 ms)	185.4 ± 44.9 (53.2 ± 37.2)	204.6 ± 69.7 (69.4 ± 50.1)	0.48 (0.42)
ARP, ms (S1S1, 120 ms)	23.5 ± 7.1	26.0 ± 13.9	0.62
AVNRP, ms (S1S1, 120 ms)	43.9 ± 9.3	50.0 ± 7.8	0.14
WBP, ms	78.0 ± 7.5	87.0 ± 7.9	0.018
	Ventricular stimulation		
VRP, ms (S1S1, 120 ms)	138.6 ± 25.8	143.9 ± 22.7	0.59
VRP, ms (S1S1, 110 ms)	449 ± 95	426 ± 61	0.46
VRP, ms (S1S1, 100 ms)	14.6 ± 2.1	15.9 ± 2.2	0.15
	Arrhythmia induction		
AF, % inducible animals	60	50	0.99
VT, % inducible animals	33.3	50	0.65

$n = 10$ for atrial simulation and 9 and 10 for ventricular simulation of $Cx30.2^{LacZ/LacZ}$ and $Cx30.2^{+/+}$, respectively. SNRP, sinus node recovery period; S1S1, basal stimulation cycle length; ARP, atrial refractory period; AVNRP, AV-nodal refractory period; WBP, Wenckebach periodicity; VRP, ventricular refractory period; AF, atrial fibrillation; VT, ventricular tachycardia.

by evaluation of the Wenckebach periodicity, which is a marker of AV-nodal conduction capacity. Wenckebach periodicity is defined as cycle length of atrial stimulation with loss of proper (1:1) AV-nodal conduction to the ventricles, resulting in cyclic AV-nodal blockade. $Cx30.2^{LacZ/LacZ}$ mice exhibited a significant lower Wenckebach periodicity as compared with their $Cx30.2^{+/+}$ littermates, which strongly indicates facilitated AV-nodal conduction, allowing transition of faster heart rates from atria to ventricles in the transgenic mouse strain (Table 2). AV-nodal refractory period at basic stimulus cycle length was not significantly reduced in the $Cx30.2^{LacZ/LacZ}$ mice. Thus, acceleration of AV conduction in the $Cx30.2^{LacZ/LacZ}$ animals seemed independent of changes in absolute refractory period of AV-nodal tissue. Furthermore, no alterations were present with regard to sinus node automaticity and atrial and ventricular refractory periods (Table 2).

Atrial burst stimulation showed no differences in inducibility of atrial fibrillation among the groups (inducible episodes per animal: 2.1 ± 1.4 in $Cx30.2^{LacZ/LacZ}$ versus 1.6 ± 1.6 in $Cx30.2^{+/+}$; $P = 0.44$). Ventricular heart rate during these induced episodes of atrial fibrillation was significantly higher in the deficient mice (600.0 ± 68.2 bpm versus 489.0 ± 70.5 in $Cx30.2^{+/+}$; $P = 0.009$) because of faster AV-nodal conduction in these atrial tachyarrhythmias. All episodes converted spontaneously, and no sustained tachyarrhythmias were observed. Ventricular vulnerability was unchanged in $Cx30.2^{LacZ/LacZ}$ mice (Table 2).

Expression of Cx40, Cx43, and Cx45 in Cx30.2-Deficient Mice. To determine whether an up-regulation of other cardiac connexines compensates the lack of Cx30.2 in the SA node, AV node and AV bundle, we performed immunofluorescence analyses in consecutive heart cryosections of $Cx30.2^{+/+}$, $Cx30.2^{+/LacZ}$, and $Cx30.2^{LacZ/LacZ}$ animals (Figs. 6–8, which are published as supporting information on the PNAS web site). Coexpression of Cx30.2 and Cx45 was found within the AV node (Fig. 6), SA node and AV bundle (Fig. 7) of $Cx30.2^{+/+}$ and $Cx30.2^{+/LacZ}$ mice. Cx40 and Cx30.2 only partially colocalized within the AV node (Fig. 6). We did not detect obvious changes in the expression levels of Cx40, Cx45, and Cx43 in the AV node (Fig. 6), the SA node, and the AV bundle (Fig. 7) of the different genotypes.

Discussion

In the mammalian heart, electrical impulses are generated by self-excitatory pacemaker cells in the SA node. Excitation is transferred with high conduction velocity to the AV node, where conduction is delayed. Subsequently, electrical impulses quickly propagate through the His-Purkinje system to the ventricular myocytes, which simultaneously contract. The myocytes of the SA node and AV node differ with respect to their morphology and connexin expression pattern from the fast conducting working myocytes of atria and ventricles and cardiomyocytes of the His-Purkinje system (17). Cell and tissue geometry and action potential parameters (e.g., dV/dt) have been described to influence the conduction velocity during cardiac impulse propagation (18–21). Furthermore, the extent of intercellular coupling and the intrinsic electrophysiological properties of the gap junction channels expressed in the different compartments of the heart are thought to contribute to the corresponding distinctive conduction velocities (17, 19, 22).

Cx channels with high unitary conductance composed of Cx40 (180 pS) and Cx43 (115 pS) (23, 24) contribute to the fast conduction through the atrial and ventricular working myocardium. In contrast, the SA node and AV node are specialized tissues with slow impulse propagation that, in wide areas, only show expression of Cx30.2 (9 pS) and Cx45 (32 pS) (14). Because of the low unitary conductance of both Cx channels, electrical coupling in the nodal tissues could be reduced, thus contributing to the slowdown of conduction (14).

In our present study, we ablated Cx30.2 in mice. We demonstrated that $Cx30.2^{LacZ/LacZ}$ mice lacking this connexin show no severe heart anomalies under normal physiological conditions. No macro- or microscopical structural abnormalities in heart morphology were found. Left ventricular function parameters investigated by echocardiography with and without dobutamine stress were unchanged.

To estimate the influence of Cx30.2 on electrophysiological characteristics of the heart action, we performed surface ECG analyses. At similar baseline heart rates, the ECG revealed a 25% shortened PQ interval in $Cx30.2^{LacZ/LacZ}$ as compared with $Cx30.2^{+/+}$ mice. Similar P wave durations in both groups pointed toward isolated AV-nodal alterations and the absence of changes in atrial conductivity as possible reasons for this phenomenon.

To examine in more detail the cardiac and, in particular, AV-nodal impulse propagation, we performed invasive *in vivo* electrophysiological investigations. During catheter positioning, Cx30.2-deficient mice frequently exhibited AV-nodal conduction blocks. This enhanced vulnerability of the AV node toward mechanical stress could not be attributed to histomorphological changes. Although the exact reasons for this finding have to be further accessed, such changes can be of pathophysiological

relevance in states of enhanced stretch in the AV-nodal region, e.g., in cardiomyopathies (25). Analyses of intracardiac electrograms confirmed surface-ECG findings of accelerated transition on the AV-nodal level. The loss of Cx30.2 resulted in a faster conduction above the His-bundle, whereas infraHisian conduction was not altered. This finding proves the presence of enhanced AV-nodal conduction in $Cx30.2^{LacZ/LacZ}$ mice.

Atrial and ventricular stimulations were performed to test the functions of the cardiac conduction parameters. Although Cx30.2 is expressed in the area of the SA node, we did not find altered impulse generation in the SA node (or evidence for sinoatrial dysfunction in the surface ECG analyses). However, a possible acceleration of impulse propagation from the SA node to the atrial myocardium cannot be investigated *in vivo*, mainly because of the small size of the affected excitable tissue, but cannot be ruled out either. This fact represents the methodological restriction of our examinations. Optical mapping methods of the SA-nodal area might be a helpful tool in further investigations addressing this interesting question. Furthermore, we could not finally clarify whether Cx30.2 immunostaining in the SA-nodal area was due to Cx30.2 expression in the nodal cells or to expression in neuronal cells of the innervation.

The alterations in AV-nodal conduction also resulted in functional disturbances. Cx30.2-deficient mice exhibited lower Wenckebach periodicity in the testing of AV-nodal transition capacity and faster AV-nodal impulse propagation and ventricular heart rate during induced episodes of atrial fibrillation. This acceleration was not accompanied by a decrease of the AV-nodal refractory period, although AV-nodal refractory period is known to usually correlate to Wenckebach periodicity in humans, yet at a low correlation coefficient (26). The reason for this finding in our mouse model remains to be clarified. Faster AV-nodal conduction properties and unchanged or even elevated AV-nodal refractory period are not a necessarily contradictory finding, but a common pathophysiological phenomenon in arrhythmias involving fast-conducting AV-nodal pathways (27, 28).

The conduction delay is supposed to be the main function of the AV node, which permits the sequential contraction of atria and ventricles (29). Furthermore, during high atrial heart rates, e.g., atrial fibrillation, the slow AV-nodal conductivity preserves the direct impulse transition to the ventricles, thus protecting the ventricular myocardium from the induction of ventricular arrhythmias like ventricular tachycardia or ventricular fibrillation (30). The factors responsible for this essential retardation of impulse propagation on AV-nodal level were largely unclear. Nevertheless, disturbances of AV-nodal conductivity are of pathophysiological and clinical relevance, such as in the formation of dual pathways with different conduction velocities (slow and fast conducting areas of the AV node) (31). Different conduction properties of AV-nodal tissue with such division into slow (short refractory period) and fast (long refractory period) pathways facilitate development of local reentry and, thus, are the pathophysiological substrate for AV-nodal reentry tachycardia, the most common congenital supraventricular tachycardia in humans (32, 33). Despite the high incidence of this tachycardia, little is known about the ultrastructural and cellular changes of the AV-nodal tissue leading to these differences in conduction velocity. This study identifies a connexin channel that slows down AV-nodal impulse propagation and might represent a factor of pathophysiological relevance in AV-nodal reentry tachycardia.

Patients suffering from the Wolff-Parkinson-White syndrome exhibit an accessory pathway, consisting of myocytal tissue typically lacking the conduction-slowing properties of the AV node. This condition can result in life-threatening ventricular tachycardias and sudden arrhythmic cardiac death due to fast conduction of supraventricular arrhythmias to the ventricles (34, 35). In analogy, induction of ventricular tacharrhythmias can be observed under accelerated AV-nodal conduction (36). Such phenomenon was also observed in Cx30.2-deficient mice, which developed higher heart rates during induced episodes of atrial fibrillation as compared with WT animals. Thus, the protective impulse retarding effect of the AV node seems to be directly dependent on the presence of Cx30.2 in this specialized tissue.

We propose that an increased junctional conductance (g_j) could lead to the enhanced conduction velocity within the AV node. Junctional conductance is depending on the total number of gap junctions and the unitary conductance of the single channels. Enhanced junctional conductance in Cx30.2-deficient mice could be obtained by two mechanisms. On the one hand, the loss of Cx30.2 might induce the up-regulation of other connexins, e.g., Cx45 and Cx40, resulting in a similar number of gap junctional channels with higher unitary conductance. However, our immunofluorenscence analyses of the cardiac connexins did not indicate obvious up-regulation of Cx45, Cx40, and Cx43 in the AV node of Cx30.2-deficient mice.

On the other hand, the removal of Cx30.2 from heterotypic/heteromeric gap junctional channels that might be formed in areas of coexpression with Cx45 and Cx40 would result in channels which exhibit a higher unitary conductance in the $Cx30.2^{LacZ/LacZ}$ mice. This property directly could lead to an increased junctional conductance and, accordingly, to a stronger coupling of the AV-nodal cells, even if the total number of gap junction channels is reduced. Heterotypic channels involving Cx30.2 were shown to exhibit very low single channel conductances (14). The deletion of Cx30.2 in mice resulted in wide areas of the AV node in gap junction channels that presumably only contain Cx45. These Cx45 homotypic channels exhibited in transfected cells a higher unitary conductance (32 pS) than homotypic Cx30.2 gap junction channels (9 pS), heterotypic gap junction channels involving Cx30.2/Cx45 (17 pS) (14, 37), and probably heteromeric Cx30.2/Cx45 gap junction channels, which might be formed in the WT heart. Thus, Cx30.2 might have a dominant negative effect on junctional conductance when included with other connexins in the same gap junctional channels.

We could not determine whether higher conduction velocity was due to the absence of Cx30.2 from heterotypic/heteromeric channels involving Cx45 or Cx40, thus enhancing, e.g., the number of Cx45 and Cx40 homotypic channels. Furthermore, the deletion of Cx30.2 might have resulted in a moderate up-regulation of Cx45 or Cx40 in the nodal tissues of the adult mouse heart below our detection level. In addition to differences in transjunctional conductance, other alterations of gap junctional intercellular communication that occur upon deletion of Cx30.2 might have affected the decrease in AV-nodal conduction velocity.

Our study identifies Cx30.2 deficiency as a condition promoting and accelerating AV-nodal conductivity in the mouse heart, thus characterizing Cx30.2 as a component responsible for conduction slowing in AV-nodal tissue. Gap junction channels of the human orthologue Cx31.9 also exhibit low unitary conductance (38, 39). Thus, its effect on conduction characteristics in human cardiac electrophysiology and AV-nodal physiology should be investigated.

Materials and Methods

Generation of Cx30.2 Transgenic Mice. Construction of the targeting vector, transfection of ES cells, and characterization of ES cells and Cx30.2 transgenic mice are described in *Supporting Materials and Methods*, which is published as supporting information on the PNAS web site. The targeting vector pMK-Cx30.2 contained a floxed (flanked by loxP sites) region that included the Cx30.2 coding sequence, the "flirted" (flanked by frt sites), phospoglycerate promoter driven neo selection cassette (PGK-neo), and downstream the floxed region a LacZ reporter gene with nuclear localization signal. After homologous recombination in ES cells and blastocyst injection, Cx30.2 transgenic mice (Cx30.2fl) were

obtained. Heterozygous Cx30.2$^{+/fl}$ males were crossed to hACT-B:FLPe females expressing the Flp-recombinase (15) to generate Cx30.2$^{+/fldN}$ and to PGK-Cre females (16) to get Cx30.2$^{+/LacZ}$ mice. The different allelic variants were verified by PCR and Southern blot analyses.

RT-PCR Analysis. RNA preparation and intron-spanning RT-PCR analyses were performed as described in ref. 14 by using Cx30.2- and LacZ-specific primers derived from the untranslated Exon1 (P1: 5′-CTC AGC TCT AAG GCC CAG GTC CCG), the Cx30.2 coding region (C-TER-DSP: 5′-CCG CGC TGC GAT GGC AAA GAG) and the LacZ reporter gene (LacZ-DSP: 5′-CCT CTT CGC TAT TAC GCC AG).

Immunocytochemistry and LacZ Staining. Adult mice hearts from different genotypes were dissected from cervically dislocated mice, frozen in the gas phase of liquid nitrogen, and cryosectioned (20 μm). Immunofluorescence analyses with Cx30.2 antibodies and LacZ staining of heart cryosections were carried out as described in refs. 11 and 14.

Electrophysiological Examination. The procedures are described in detail in *Supporting Materials and Methods*. Preparation and catheterization of the jugular vein and electrophysiological investigation of adult mice were performed under inhalative anesthesia (1.5 vol% isoflurane in 70% N_2O/30% O_2) at a constant body temperature of 37°C. Our analyses included intracardiac atrial and ventricular stimulation. Baseline ECG (R-R interval, P wave duration, PQ interval, QRS duration, and QT interval) and electrophysiologic parameters (sinus node refractory period, Wenckebach periodicity, AV-nodal refractory period, and AV-conduction properties) were evaluated. Inducibility and incidence of atrial and ventricular tachyarrhythmias were tested by using programmed (up to three short-coupled extra beats) and burst stimulation protocols as described in ref. 40. To estimate AV-nodal pulse propagation to the ventricles during atrial tachycardias, ventricular frequency was analyzed during the induced episodes of atrial fibrillation.

We thank Gerda Hertig for technical help with the characterization of the Cx30.2-deficient mice. This work was supported by German Research Association Grants WI 270/24-1,2 and WI 270/22-5,6 (to K.W.), Bonn University Grant BONFOR O-109.0008 (to J.W.S.), and an internal grant from Bonner Forum Biomedizin (to K.W.).

1. Kumar, N. M. & Gilula, N. B. (1996) *Cell* **84,** 381–388.
2. Neijssen, J., Herberts, C., Drijfhout, J. W., Reits, E., Janssen, L. & Neefjes, J. (2005) *Nature* **434,** 83–88.
3. Söhl, G. & Willecke, K. (2004) *Cardiovasc. Res.* **62,** 228–232.
4. Gros, D. B. & Jongsma, H. J. (1996) *BioEssays* **18,** 719–730.
5. Beyer, E. C., Kistler, J., Paul, D. L. & Goodenough, D. A. (1989) *J. Cell Biol.* **108,** 595–605.
6. Reaume, A. G., De Sousa, P. A., Kulkarni, S., Langille, B. L., Zhu, D., Davies, T. C., Juneja, S. C., Kidder, G. M. & Rossant, J. (1995) *Science* **267,** 1831–1834.
7. van Rijen, H. V., van Veen, T. A., van Kempen, M. J., Wilms-Schopman, F. J., Potse, M., Krüger, O., Willecke, K., Opthof, T., Jongsma, H. J. & de Bakker, J. M. (2001) *Circulation* **103,** 1591–1598.
8. Kirchhoff, S., Nelles, E., Hagendorff, A., Krüger, O., Traub, O. & Willecke, K. (2000) *Curr. Biol.* **8,** 299–302.
9. Verheijck, E. E., van Kempen, M. J., Veereschild, M., Lurvink, J., Jongsma, H. J. & Bouman, L. N. (2001) *Cardiovasc. Res.* **52,** 40–50.
10. Coppen, S. R., Dupont, E., Rothery, S. & Severs, N. J. (1998) *Circ. Res.* **82,** 232–243.
11. Krüger, O., Plum, A., Kim, J. S., Winterhager, E., Maxeiner, S., Hallas, G., Kirchhoff, S., Traub, O., Lamers, W. H. & Willecke, K. (2000) *Development (Cambridge, U.K.)* **127,** 4179–4193.
12. van Rijen, H. V., Eckardt, D., Degen, D., Theis, M., Ott, T., Willecke, K., Jongsma, H. J., Opthof, T. & de Bakker, J. M. (2004) *Circulation* **109,** 1048–1055.
13. Nishii, K., Kumai, M., Egashira, K., Miwa, T., Hashizume, K., Miyano, Y. & Shibata, Y. (2003) *Cell Commun. Adhes.* **10,** 365–369.
14. Kreuzberg, M. M., Söhl, G., Kim, J. S., Verselis, V. K., Willecke, K. & Bukauskas, F. F. (2005) *Circ. Res.* **96,** 1169–1177.
15. Rodríguez, C. I., Buchholz, F., Galloway, J., Sequerra, R., Kasper, J., Ayala, R., Stewart, A. F. & Dymecke, S. M. (2000) *Nat. Genet.* **25,** 139–140.
16. Lallemand, Y., Luria, V., Haffner-Krausz, R. & Lonai, P. (1998) *Transgenic Res.* **7,** 105–112.
17. Severs, N. J. (2001) *J. Cell. Mol. Med.* **5,** 355–366.
18. Spach, M. S., Heidlage, J. F., Dolber, P. C. & Barr, R. C. (2000) *Circ. Res.* **86,** 302–311.
19. Kléber, A. G. & Rudy, Y. (2004) *Physiol. Rev.* **84,** 431–488.
20. Kucera, J. P. & Rudy, Y. (2001) *Circ. Res.* **89,** 799–806.
21. Kucera, J. P., Kléber, A. G. & Rohr, S. (1998) *Circ. Res.* **83,** 795–805.
22. Rohr, S., Kucera J. P. & Kléber, A. G. (1998) *Circ. Res.* **83,** 781–794.
23. Bukauskas, F. F., Elfgang, C., Willecke, K. & Weingart, R. (1995) *Biophys. J.* **68,** 2289–2298.
24. Bukauskas, F. F., Bukauskiene, A., Bennett, M. V. & Verselis, V. K. (2001) *Biophys. J.* **81,** 137–152.
25. Otomo, J., Kure, S., Shiba, T., Karibe, A., Shinozaki, T., Yagi, T., Naganuma, H., Tezuka, F., Miura, M., Ito, M., *et al.* (2005) *J. Cardiovasc. Electrophysiol.* **16,** 137–145.
26. Bissett, J. K., Kane, J. J., De Soyza, N. & Murphy, M. L. (1975) *Cardiovasc. Res.* **9,** 593–599.
27. Moe, G. K., Preston, J. B. & Burlington, H. (1956) *Circ. Res.* **4,** 357–362.
28. Rosen, K. M., Mehta, A. & Miller, R. A. (1974) *Am. J. Cardiol.* **33,** 291–298.
29. Mazgalev, T. N. & Tchou, P. J. (2000) *Atrial-AV Nodal Electrophysiology: A View from the Millenium* (Futura Publishing, New York).
30. Dobrzynski, H., Nikolski, V. P., Sambelashvili, A. T., Greener, I. D., Yamamoto, M., Boyett, M. R. & Efimov, I. R. (2003) *Circ. Res.* **93,** 1102–1110.
31. Efimov, I. R., Nikolski, V. P., Rothenberg, F., Greener, I. D., Li, J., Dobrzynski, H. & Boyett, M. (2004) *Anat. Rec. A Discov. Mol. Cell Evol. Biol.* **280,** 952–965.
32. Akhtar, M., Jazayeri, M. R., Sra, J., Blanck, Z., Deshpande, S. & Dhala, A. (1993) *Circulation* **88,** 282–295.
33. Jackman, W. M., Beckman, K. J., McClelland, J. H., Wang, X., Friday, K. J., Roman, C. A., Moulton, K. P., Twidale, N., Hazlitt, H. A., Prior, M. I., *et al.* (1992) *N. Engl. J. Med.* **327,** 313–318.
34. Waspe, L. E., Brodman, R., Kim, S. G. & Fisher, J. D. (1986) *Am. Heart J.* **112,** 1141–1152.
35. Wellens, H. J. & Durrer, D. (1974) *Am. J. Cardiol.* **34,** 777–782.
36. Wang, Y. S., Scheinman, M. M., Chien, W. W., Cohen, T. J., Lesh, M. D. & Griffin, J. C. (1991) *J. Am. Coll. Cardiol.* **18,** 1711–1719.
37. Bukauskas, F. F., Angele, A. B., Verselis, V. K. & Bennett, M. V. L. (2002) *Proc. Natl. Acad. Sci. USA* **99,** 7113–7118, and erratum (2002) **99,** 10228.
38. Nielsen, P. A., Beahm, D. L., Giepmans, B. N., Baruch, A., Hall, J. E. & Kumar, N. M. (2002) *J. Biol. Chem.* **277,** 38272–38283.
39. White, T. W., Srinivas, M., Ripps, H., Trovato-Salinaro, A., Condorelli, D. F. & Bruzzone, R. (2002) *Am. J. Physiol.* **283,** C960–C970.
40. Schrickel, J., Bielik, H., Yang, A., Schimpf, R., Shlevkov, N., Burkhardt, D., Meyer, R., Grohe, C., Fink, K., Tiemann, K., *et al.* (2002) *Basic Res. Cardiol.* **97,** 452–460.